Cement and Concrete Research 38 (2008) 1306–1314

Contents lists available at ScienceDirect

Cement and Concrete Research

journal homepage: http://ees.elsevier.com/CEMCON/default.asp

On the frictional contribution to the viscosity of cement and silica pastes in the presence of adsorbing and non adsorbing polymers

H. Lombois-Burger [a], P. Colombet [a], J.L. Halary [b], H. Van Damme [b,*]

[a] CTG Italcementi Group, rue des Technodes, F-78931 Guerville cedex, France
[b] Ecole Supérieure de Physique et de Chimie Industrielles, PPMD Laboratory, UMR 7615 CNRS-ESPCI-UPMC, 10 rue Vauquelin, 75231 Paris cedex 05, France [1]

ARTICLE INFO

Article history:
Received 1 March 2007
Accepted 22 August 2008

Keywords:
Cement pastes
Silica
Rheology
Friction
Polymer

ABSTRACT

This paper is devoted to the role of hydrodynamic lubrication in the flow of dense suspensions of non-Brownian cement or silica particles. The role of hydrodynamic lubrication is ambiguous since it is primarily a source of viscous dissipation but, by preventing direct contact between particles and friction, it may facilitate flow. We show that in the concentration and shear rate regimes investigated here direct contact friction between cement or silica particles is contributing to the overall energy dissipation. Addition of water-soluble polymers, either adsorbing or not adsorbing, was used as a mean to control friction. We show that, independently of the adsorption capacity of the polymer, it is the non adsorbed polymer which, thanks to hydrodynamic lubrication, prevents direct contacts and reduces the overall energy dissipation. This leads to the counterintuitive situation where by increasing the interstitial fluid viscosity, the suspension viscosity is decreased. When hydrodynamic lubrication is no longer able to avoid direct frictional contact, dilatant and shear-thickening behaviors set in.

1. Introduction

Fresh cement pastes belong to a class of particulate fluids which are intermediate between concentrated colloidal suspensions and coarse granular media. The rheological behavior of the former is dominated by non contact surface forces (van der Waals, double layer, steric forces) and by hydrodynamic dissipation [1]. In concentrated colloidal suspensions, hydrodynamic dissipation is mainly due to the expulsion of the interstitial fluid as two particles approach each other. This is the so-called hydrodynamic lubrication [2]. On the other hand, in coarse granular media like geological debris flow, hydrodynamic lubrication may become ineffective in preventing direct contact, due to the strong inertial forces. Collisions and friction plays then the essential role [3,4].

This brief introduction highlights the ambiguous role that hydrodynamic lubrication may play in the flow of dense granular media. On the one hand, it is definitely a source of dissipation but, on the other hand, by preventing direct interparticle contact and friction, it may facilitate flow. Whereas the role of friction is well recognized in concrete and coarse slurries [5,6], it is much less so in cement pastes. Important rheological properties like the yield stress [7,8] or the thixotropic behavior [9,10] are usually interpreted in terms of non contact interactions. In a recent paper devoted to kneading and extrusion of dense polymer-cement pastes, we have shown that hydrodynamic lubrication due to the interstitial polymer solution is the relevant parameter for facilitating the flow in the extruder contraction and die land [11]. The adsorbed polymer was found to be inoperative. The purpose of the present paper is to go deeper in the investigation of friction and lubrication phenomena, in cement and crushed silica pastes in simple flow geometries, that is, in rheometric flows. Like in our previous paper, we choose to compare adsorbing and non adsorbing polymers. The polymers which were used do not belong to classical superplasticizers families. They were selected on the basis of other criteria, as their effectiveness in conferring plasticity to the paste and preventing filtration and dilatancy during extrusion. As will be shown below, depending on the shear rate, hydrodynamic lubrication may or may not avoid direct contact. In the former case, at low shear rate, only the non adsorbed part of the polymer is involved. In the latter case, shear-thickening is observed and friction is controlled by the adsorbed polymer or by the bare surface.

2. Materials and methods

2.1. Materials

Two types of particles were used: ordinary Portland cement and silica. The ordinary Portland cement (CEM I 42.5) was obtained from Italcementi Group, with the following characteristics: Bogue composition, determined from X-ray fluorescence analysis (*w*%): C_3S (56.2%), C_2S (20.2%), C_3A (0.%), C_4AF (16.2%); Blaine surface area: 3680 cm^2/g;

* Corresponding author. Tel.: +33 1 40 79 44 19; fax: +33 1 40 79 46 86.
E-mail address: henri.vandamme@espci.fr (H. Van Damme).
[1] PPMD laboratory, UMR 7615 CNRS-ESPCI-UPMC.

0008-8846/$ – see front matter © 2008 Elsevier Ltd. All rights reserved.
doi:10.1016/j.cemconres.2008.08.002

average particle diameter, in number: 15 μm; density: 3.2 g/cm^3. The silica (crushed cristobalite), with a specific surface area of 4700 cm^2/g, an average particle diameter of 10 μm and a density of 2.3 g/cm^3, was purchased from Sibelco. The solid volume fraction in the pastes was varied from 0 to 0.55.

Two polymers were used, with relatively high molecular masses: (i) a random acrylic copolymer synthesized by ATO (now Arkema), hereafter referred to as PA, (M_v = 3.10^5 g/mol) containing 45% (w/w) of methacrylic acid and 55% (w/w) of ethyl acrylate; (ii) poly(ethylene oxide) from Aldrich (M_v = 2.10^6 g/mol, $R_g \cong$ 50 nm), referred to as PEO. As mentioned in the Introduction section, they were selected on the basis of their effectiveness in conferring plasticity to the paste and preventing filtration and dilatancy during extrusion. PA was always used in its pre-neutralised form, i.e. with one mole of NaOH per mole of methacrylic acid monomer. All polymer solutions were homogenized for at least 12 h before use. An important difference between the polymers lies in their ability to adsorb or not on the cement or silica particles. As will be shown later, PEO does not adsorb on cement but does adsorb on silica through hydrogen bonding with the surface OH groups [12]. Conversely, PA adsorbs on cement but not on silica.

2.2. Adsorption isotherms

In order to quantify the interaction between the polymers and the hydrating cement particles and the silica, the adsorption isotherms of each polymer were measured at room temperature. The paste samples were prepared with a constant water to solid weight ratio, w/s = 0.60, and variable polymer concentrations in the aqueous phase. The pastes were prepared by mixing the polymer solution with the solid (cement or silica) using a helix mixer. Mixing was performed for 1 min at low speed (100 rpm) and for 2 min at high speed (400 rpm), after which the pastes were allowed to rest. Ten min after the beginning of mixing, the interstitial solution was extracted by centrifugation and the carbon content determined by total organic carbon analysis, after dilution of the supernatant and removal of dissolved carbon dioxide by flowing N_2 into the solution. The contact time (10 min) was chosen in order to avoid too much interference with the hydration reaction. As explained in the next section, the rheological measurements were started at about the same time. Thus, even by adding the duration of the rheological measurements (~15 min at most), we are still within the dormant period. The results were corrected for the carbon contained in the water and in the cement or silica particles. The quantity of polymer adsorbed was calculated from the difference between the carbon content in solution before and after contact with cement or silica. Lengthening the contact time up to one hour led only to a ~10% increase of the amount adsorbed. With PEO and silica, adsorption was measured at ~pH 6. This is far above the point of zero charge of quartz (~1). Thus, adsorption should be only marginally sensitive to possible small pH changes.

2.3. Rheological measurements

Silica and cement pastes of given polymer to water (p/w) weight ratio were prepared by mixing the polymer solution with the solid (cement or silica) as explained in Section 2.2. The volume fractions of the pastes were calculated using the known density of the cement and the measured (PA) or calculated (PEO) density of the polymer solutions. These volume fractions will be referred as ϕ for both cement and silica pastes.

We used an AR1000 N controlled stress Rheometer equipped with a normal force transducer from TA Instruments. A 40 mm plane-plane tool with a gap of 1700 μm (more than ten times larger than the larger particles) was used. Both the upper and lower planes were ridged to avoid any slipping at the interface between the tool and the sample. A water trap was used to avoid evaporation above the sample.

A widespread procedure in the rheological study of pastes is to pre-shear the sample before performing the measurements, in order to "erase" the history of the material. In our case, it was observed that a pre-shear was inducing the cohesive fracture of the sample (that is, fracture in the bulk of the paste layer). For that reason, no pre-shear was performed, but the samples were allowed to rest for at least 3 min in the rheometer in order to relax the stresses due to the loading of the sample. The measurement procedure starts 13 min after the beginning of mixing and consists of a non-equilibrium stress sweep from 8.10^{-3} to 7950 Pa in 15 min, with a logarithmic distribution of stress values. As compared to point-by-point equilibrium measurements, this insured that all the samples were experiencing the same ageing during the measurements. The relatively short duration of these measurements enabled us to remain in the dormant period of the cement and to limit the chemical evolution during measurements.

3. Results and discussion

3.1. Adsorption isotherms

The adsorption isotherms obtained by plotting the mass of polymer adsorbed per unit mass of cement versus the weight concentration of polymer in the interstitial solution at pseudo-equilibrium ("pseudo" because hydration is taking place, though very slowly in polymer-containing solutions) are represented in Fig. 1. For the cement/PEO and silica/PA pastes, the carbon concentrations in solution before and after mixing with cement were the same, within experimental error, which means that no adsorption occurs. The absence of adsorption of PEO on cement has already been reported and interpreted in terms of the inability of PEO molecules to hydrogen bond to the highly ionic cement surface [11–13]. On the contrary, for

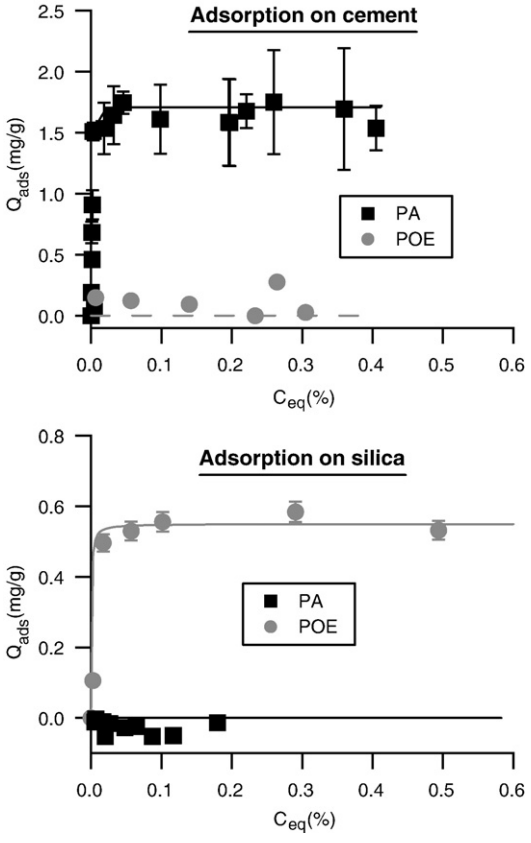

Fig. 1. Mass of polymer adsorbed per unit mass of solid as a function of the weight concentration of polymer in the interstitial fluid at equilibrium.

the cement/PA and silica/PEO pastes, the isotherms are characteristic of a high affinity mono-layer adsorption which can be correctly fitted with a Langmuir isotherm, $Q=Q_0(KC/(1+KC))$. The affinity constants K (g aqueous phase/g polymer) and plateau values Q_0 (mg polymer/g solid) are 40,500±500 and ≈1.7 for cement/PA, and 16,000±4000 and 0.6 for silica/PEO, respectively (Fig. 1). Thus, for each polymer considered, the adsorption behavior is reversed when passing from silica to cement and vice-versa.

The purpose of this paper is not to go deeper into the analysis of adsorption. As far as rheological behavior is concerned, it is enough to conclude that, for each solid, we have a polymer which is present in the interstitial solution only (PEO with cement; PA with silica) and one (PA with cement; PEO with silica) which is present in the solution *and* on the solid surface.

3.2. General rheological behavior

In spite of the differences just mentioned (adsorbing polymer *vs* non adsorbing polymer), the same general behavior is observed, as far as the (τ, $\dot{\gamma}$) or (τ, γ) diagrams are concerned. In the following, they will be called the rheological and the mechanical diagrams, respectively. Three main regimes may be identified. They are illustrated in Figs. 2 and 3 for the cement/PA and cement/PEO couples as examples.

- A low stress regime, in which the stress increases linearly with strain without significant increase of the shear rate (the parameters of this regime are in the limit working conditions of the instrument and cannot be analyzed accurately). This corresponds to the elastic response domain below the yield stress.
- A second regime in which the increase of shear stress *vs* strain levels off while the shear rate begins to increase. This corresponds to the onset of flow.
- A high stress regime in which the stress increases very slowly while shear rate and strain increase tremendously.

The interpretation of the third regime is not obvious. Visual inspection of the most concentrated pastes pointed towards the occurrence of cohesive fracture in the rheometer gap. In order to confirm this interpretation, we compared the mechanical and flow curves of non-pre-sheared cement/PA pastes with those of pre-sheared pastes (Figs. 4 and 5). Pre-shearing was applied for 30 s, just before the 3 min rest time at the beginning of the rheological test, at a given stress level τ_o that was varied in order to explore the three domains previously defined. If τ_o is in the first low stress regime (τ_o=10 Pa), neither the rheological nor the mechanical response is changed by the pre-shear step. This confirms that the first zone is an elastic one. If τ_o is in the second regime (τ_o=250 Pa), the rheological response is still unchanged but the mechanical response is decreased (larger strain for a given stress value). In other words, the yield point was overcome, so that a permanent strain remains. However, the strain field seems to remain homogeneous (no localization) since the rheological answer is unchanged. Finally, when τ_o is in the third regime, a pre-shear induces both a rheological and a mechanical response much lower than those of a non-pre-sheared paste, indicating that the sample was macroscopically fractured.

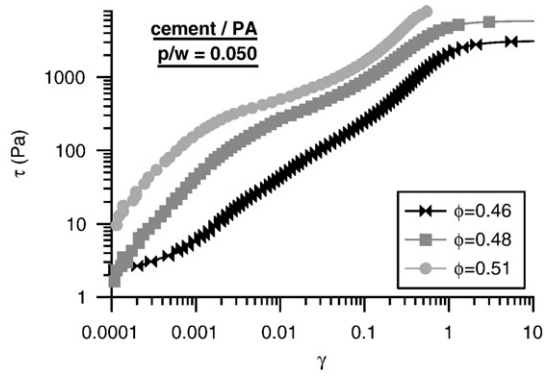

Fig. 2. Shear stress *vs* shear strain curves for cement/PA pastes at p/w=0.050.

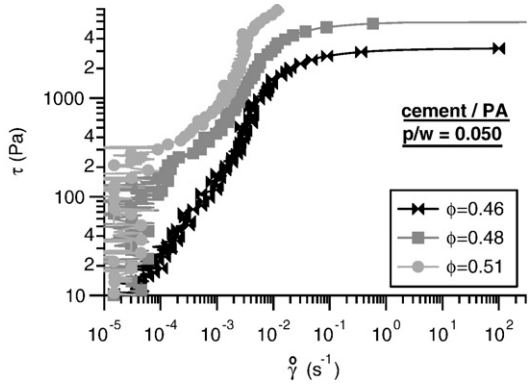

Fig. 3. Shear stress *vs* shear rate curves for cement/PA pastes at p/w=0.050.

Several regimes may also be identified when the apparent viscosity is plotted *vs* shear rate (Figs. 6 and 7). When the polymer adsorbs on the solid (silica-PEO and cement-PA, Fig. 6), a Newtonian regime is observed first at very low shear rate, below ≅10^{-3} s^{-1}, corresponding to the onset-of-flow regime in the (τ, $\dot{\gamma}$) diagram. When it does not adsorb (cement-PEO, Fig. 7, and silica-PA), this initial Newtonian regime is replaced by a shear-thinning regime. In both cases – with or without adsorption – this initial regime is often followed by a shear-thickening regime over a relatively narrow range of shear rates (less than a decade). Finally, at still higher shear rates (above≅10^{-2} s^{-1}), beyond a peak value which will be called the "shear-thickening bump" in the following, a strongly shear-thinning is observed in all cases. This corresponds to the fracturing regime discussed above. This regime, in which it was visually observed that some paste is ejected from the rheometer gap, will not be considered further.

In the following we will first analyze the polymer concentration and nature dependence of the yield stress. The flow behavior at low and high shear will be analyzed next.

3.3. Yield stress

Several methods can be used to determine a yield stress. A first method is to fit the data with a suitable model like the Herschel–Buckley model ($\tau=\tau_\gamma+\eta\dot{\gamma}^n$). However, this is questionable in the present case due to the large noise on $\dot{\gamma}$ close to the lower limit of the

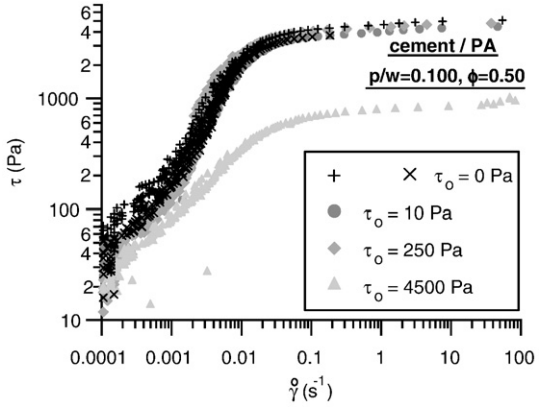

Fig. 4. Influence of a 30 s pre-shear at shear stress τ_o on the rheological curve of a PA containing cementitious paste of p/w=0.100 and ϕ=0.50.

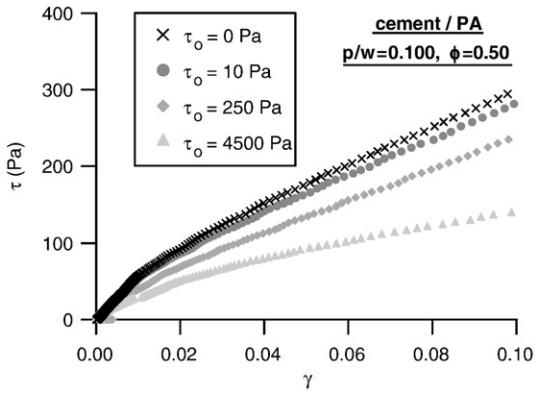

Fig. 5. Influence of a 30 s pre-shear at shear stress τ_o on the mechanical curve of a PA containing cementitious paste of $p/w=0.100$ and $\phi=0.50$.

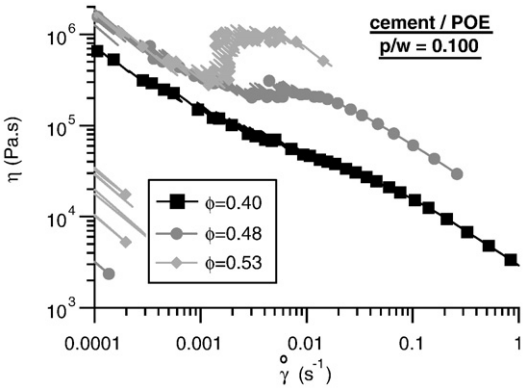

Fig. 7. Evolution of viscosity with shear rate in a polymer non-adsorbing system (PEO containing cementitious pastes of $p/w=0.100$).

instrument ($\cong 10^{-4}\,s^{-1}$). In addition the range over which the fit can be adjusted is quite narrow. A second method, which is more accurate in the present case and which was used, is to determine a plasticity yield stress (τ_y, γ_y) on the shear stress-shear strain curves. This yield point is set as the intersection between the elastic linear regime and the straight line describing plastic flow between the yield point and $\gamma=0.05$.

For all the systems considered, τ_y so determined increases with the cement or silica volume fraction, for a given p/w value (Fig. 8). The stress required to go beyond the elastic zone is all the more important as the mineral loading is higher. Conversely, the plastic strain γ_y, which ranges typically from 0.04 to 0.0025, is decreasing when the solid content is increasing (Fig. 9). When taken together, these evolutions correspond to the behavior of a material which becomes stiffer but which, at the same time, generates all the more easily microscopic shear planes as its solid content increases.

3.4. Flow at very low shear rate

As mentioned above, the pastes exhibit an initial Newtonian behavior with viscosity η_N when the polymer adsorbs on the solid and a shear-thinning behavior when it does not adsorb. This may readily be interpreted in terms of the deflocculation induced by the adsorbed polymer molecules in the former case, and by the progressive shear-induced deflocculation in the later case. In order to compare the viscosity values of the Newtonian and the shear-thinning pastes, a choice of conditions has to be made for the cement-PEO and silica-PA pastes. Our choice was to use the narrow quasi-constant viscosity range, just before the shear-thickening bump. It is likely that this pseudo-Newtonian viscosity (η_{pN}) range is the result of a dynamic equilibrium between deflocculation and the process responsible for shear-thickening.

The Newtonian or pseudo-Newtonian viscosities have been plotted *vs* particles volume fraction for different p/w ratios in Figs. 10–13. The data were fitted using Krieger–Dougherty relationship [14]:

$$\eta^* = \frac{\eta}{\eta_o} = \left(1 - \frac{\phi}{\phi_m}\right)^{-\alpha} \tag{1}$$

The values of α and ϕ_m are tabulated in Table 1. Interestingly, for each solid, the ϕ_m values are higher for the adsorbing polymers (PA for cement and PEO for silica) than for the non adsorbing polymers. This is the signature of the deflocculating action of the adsorbed polymers. Another conclusion which may be drawn from this is the fact that the pseudo-Newtonian plateau in the case of the non-adsorbing polymers is indeed not a true Newtonian plateau. If it was, a higher ϕ_m value, equal to that of the adsorbing polymers would have been obtained. The α values will be discussed later.

For non-adsorbing systems (Fig. 10 for cement/PEO and Fig. 11 for silica/PA), the viscosity increases with polymer concentration at all solid contents, but the concentration dependence is stronger at low solid content. The increase of η_{pN} with polymer concentration may readily be interpreted in terms of classical suspensions rheology. Indeed, all classical relationships as Einstein's [15], Bachelor's [15] or Krieger–Dougherty's [14], are of the following form:

$$\eta = \eta_0 f(\phi) \tag{2}$$

Thus, the viscosity of a suspension is directly proportional to the viscosity of the suspending fluid, in agreement with a wealth of

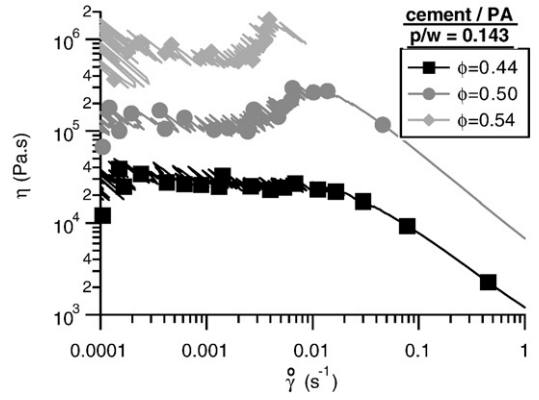

Fig. 6. Evolution of viscosity with shear rate in a polymer adsorbing system (PA containing cementitious pastes of $p/w=0.143$).

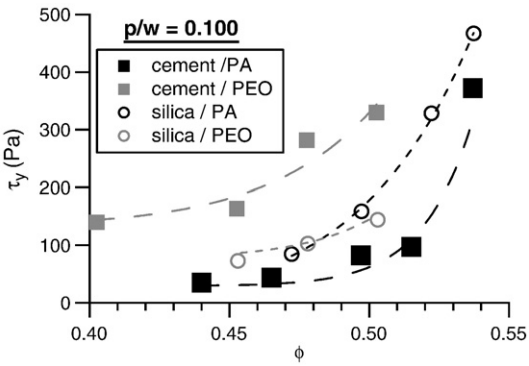

Fig. 8. Plastic yield stress versus mineral volume fraction for pastes of $p/w=0.100$.

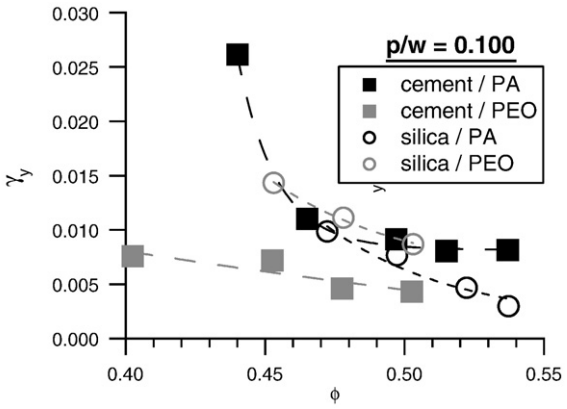

Fig. 9. Plastic yield strain versus mineral volume fraction for pastes of p/w=0.100.

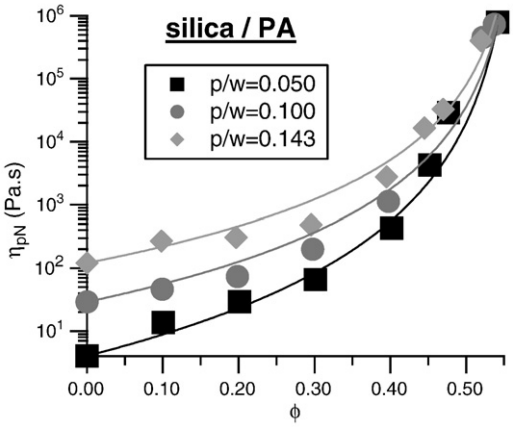

Fig. 11. Pseudo-Newtonian viscosity versus silica volume fraction of PA containing silica pastes of varying p/w ratio (polymer non-adsorbing system).

experimental observations including ours. In physical terms, this stems from the hydrodynamic nature of the dissipative processes in the flowing suspension. Less obvious is the decrease of the polymer concentration dependence at large solid content. We will return to this later.

For adsorbing polymers systems (Fig. 12 for cement/PA and Fig. 13 for silica/PEO), a surprising behavior is observed. At low solid content, nothing is changed with respect to non-adsorbing polymer systems, but at high solid content, the opposite behavior is observed. The viscosity η_N is decreasing when the polymer concentration increases. Remarkably, a relatively well-defined crossing point between the low and the high solid content regimes may be identified. This "abnormal" behavior is a key point of the present work and will be extensively discussed in the following sections.

Quite obviously, the decrease of the paste viscosity with increasing polymer concentration at high ϕ cannot be explained in the same terms as above. *A priori*, deflocculation due to the adsorbed molecules has to be considered as a possible explanation. Actually, this can be ruled out for the following reasons. First, the concentration of polymer is always much larger than the concentration needed to reach the plateau of the adsorption isotherm. Thus, the particles surface is always covered at saturation by the polymer molecules. Second, the system is most probably not flocculated since it exhibits Newtonian behavior. A flocculated suspension should be shear-thinning. However, this argument is valid only if the system is in "equilibrium" at the shear rate considered. A rough estimate of the relaxation time from the viscosity and shear modulus values G' is 0.6 s, which is slightly shorter than the time (1 s) required for obtaining one data point in the viscosity measurements. Thus, the "equilibrium" conditions are satisfied.

In agreement with previous investigations on the yield stress [16], a more relevant explanation has to be looked for in the role of interparticle contacts and solid friction in cement paste rheology [17]. While solid-solid contacts and friction are widely recognized to control the rheology of fresh concrete [5,6], they are generally overlooked in the case of cement pastes [18,19]. Yet, it was shown that, beyond a critical solid volume fraction, the yield stress of C_3S pastes had an increasing contribution of frictional forces. The hypothesis considered here is that interparticle friction is also contributing to energy dissipation, hence to the apparent viscosity. If this happens to be the case, then the lubrication effect due to the polymer might provide a reasonable explanation. This lubrication effect might stem either from the adsorbed polymer (contact lubrication) or from the polymer remaining in solution (hydrodynamic lubrication), or both. The action of the adsorbed polymer and contact lubrication may be discarded for the same reasons as those discussed above for deflocculation: since the polymer concentration is always well above the plateau of the adsorption isotherm, no evolution is expected when increasing the polymer concentration, contrary to what is observed. Hence, we are left with the hypothesis that the lubrication involved is of hydrodynamic nature.

The data also suggest that hydrodynamic lubrication is already active below the crossing point of the viscosity *vs* solid volume fraction curves. Indeed, as illustrated in Figs. 12 and 13, the gap between the viscosity curves at high and low p/w is narrowing as the

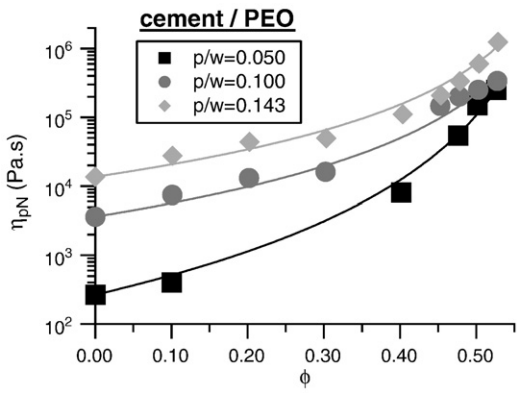

Fig. 10. Pseudo-Newtonian viscosity versus cement volume fraction of PEO containing cementitious pastes of varying p/w ratio (polymer non-adsorbing system).

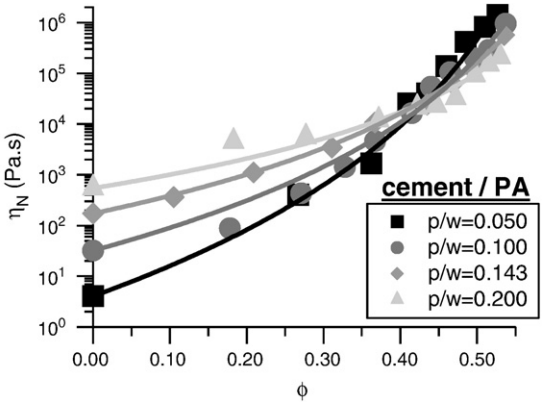

Fig. 12. Newtonian viscosity versus cement volume fraction of PA containing cementitious pastes of varying p/w ratio (polymer adsorbing system).

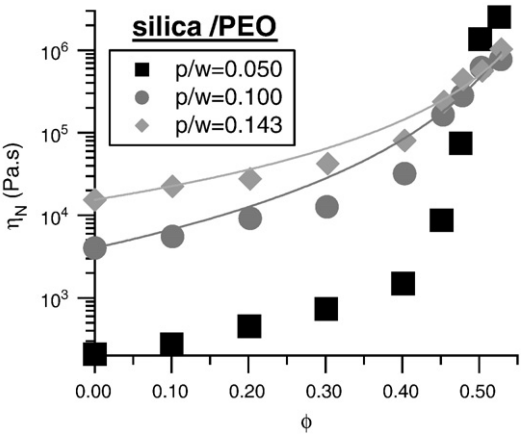

Fig. 13. Newtonian viscosity versus silica volume fraction of PEO containing silica pastes of varying p/w ratio (polymer adsorbing system).

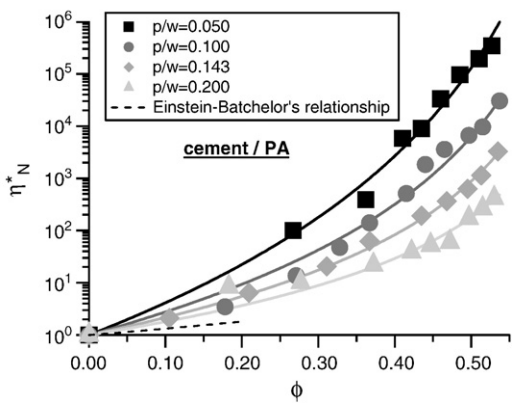

Fig. 14. Newtonian relative viscosity versus cement volume fraction for PA containing cementitious pastes of varying p/w ratio (polymer adsorbing-system).

solid volume fraction increases, that is, as the number of possible interparticle contacts increases.

If hydrodynamic lubrication is the active dissipation reduction mechanism, then it should also be effective with non-adsorbing polymers (cement/PEO and silica/PA). Indeed, as shown in Figs. 10 and 11, the same narrowing of the gap between the viscosity curves is observed at increasing solid volume fraction. However, the solid volume fraction range is not wide enough to lead to the crossing point observed with the adsorbing polymers. This may be due to the more flocculated structure of the former systems. Indeed, a population of flocs should have fewer mobile (that is, inter-floc) contacts than a population of individual (and smaller) particles.

Another point in favor of hydrodynamic lubrication is the decrease of the α parameter of Krieger–Dougherty relationship (Table 1) as the polymer concentration increases, whether the polymer is adsorbing or not. If it were contact lubrication, only the adsorbing systems would have shown an evolution of the α parameter.

In order to separate the "trivial" effect of the suspending fluid viscosity Eq. (1) from its effect on the interparticle hydrodynamic lubrication, relative viscosities, $\eta_N{}^*$ for adsorbing polymers and $\eta_{pN}{}^*$ for non-adsorbing polymers, were calculated by renormalizing the paste viscosity with respect to the viscosity of the suspending polymer solution. Strictly speaking, this viscosity should be measured in a solution with the same ionic content and force as the interstitial paste solution. For practical reasons, this was not done. One difficulty is the extremely slow dissolution kinetics of a dry polymer, especially PA. Another difficulty is the variation of the cement interstitial solution with cement content. We used the viscosities of polymer solutions in deionized water as reference. This is of no consequence for silica, considering the very low solubility of silica in our pH conditions, but it might *a priori* matter in the cementitious pastes with negatively charged polymers (PA). At high ionic strength, some screening of the charged groups will reduce the electrostatic polymer persistence length and the solution viscosity. Meanwhile, calcium-induced reticulation can also occur, which increases the solution viscosity. Hence, some compensation may be expected. In any case, the viscosity difference, if any, should be weak. We will come back to this later.

As illustrated in Fig. 14 for cement/PA and in Fig. 15 for cement/PEO, when the *relative* viscosities are considered, addition of increasing amounts of polymer leads invariably to a decrease of the relative viscosity. Thus, increasing the viscosity of the interstitial solution leads invariably to a decrease of the paste relative viscosity, whether the polymer is adsorbing or not. This behavior is observed over the whole solid volume fraction range that we explored, from 0 to ≅0.55. This confirms the hypothesis that in the granular pastes that we studied, not all the energy dissipation stems from the flow of the suspending liquid around the solid particles, like in colloidal suspensions. Interparticle contacts and friction contribute significantly to the apparent viscosity, like in dry granular media or in geological debris flow [3]. As the interstitial solution is made more viscous, it is increasingly difficult to expel this fluid from the interparticle gaps. As a consequence, fewer particles succeed in touching each other directly and the overall frictional dissipation is reduced.

As a first order attempt to correlate more quantitatively the relative viscosities to the parameters controlling hydrodynamic lubrication, we looked for a parameter which, for each polymer concentration and for each solid volume fraction, would allow us to quantify the amount of polymer active in the lubrication process. We choose the product $e\phi_p{}^{sol}$ which might be called the "effective lubrication length" (in our previous paper, we called it the "interfacial rate of active polymer"). In this product, e is the average surface-to-surface distance between particles and ϕ_p^{sol} the polymer concentration in the interstitial

Table 1
Parameters of the Krieger–Dougherty model fitting the variations of the Newtonian or pseudo-Newtonian relative viscosity

		Cement		Silica	
		PA	PEO	PA	PEO
	ϕ_m	0.67	0.63	0.57	0.63
p/w=0.050	α	8.5	3.8	4.1	–
p/w=0.100		6.4	2.6	3.4	3.0
p/w=0.143		5.0	2.4	3.1	2.2
p/w=0.200		3.8			

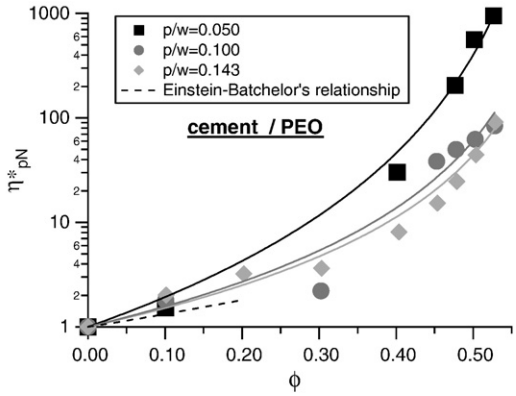

Fig. 15. Pseudo-Newtonian relative viscosity versus cement volume for PEO containing cementitious pastes of varying p/w ratio (polymer non-adsorbing system).

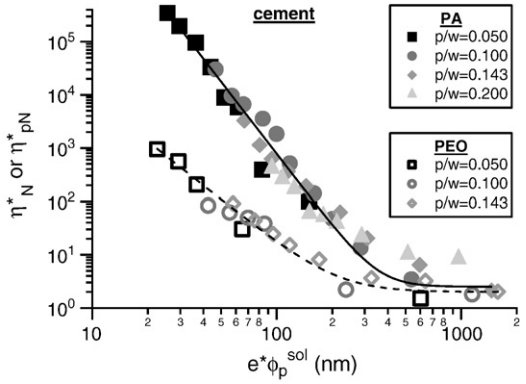

Fig. 16. Newtonian or pseudo-Newtonian relative viscosity *vs* effective lubrication length for cementitious pastes of varying *p*/*w* ratio containing an adsorbing (PA) or non-adsorbing (PEO) polymer.

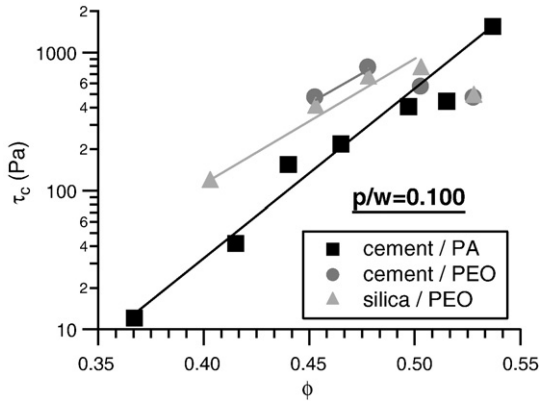

Fig. 18. Critical stress at the onset of shear-thickening, τ_c, *vs* mineral particles volume fraction, for $p/w=0.100$.

solution. Thus, the product $e\phi_p^{sol}$ is the average amount of polymer in solution in the gap separating two particles. The rationale behind this choice is that the efficiency of hydrodynamic lubrication should be related – though probably not in a linear way – to the amount of fluid between the particles and to the viscosity of this interstitial fluid.

The distance e may be calculated by dividing the volume of dispersing fluid in excess with respect to paste saturation, by half the Blaine surface area of the cement particles [11]:

$$e = \frac{2}{\rho \Sigma_B}\left(\frac{1}{\phi} - \frac{1}{\phi_m}\right) \tag{3}$$

where ρ, Σ_B and ϕ_m are the specific gravity, the Blaine surface area and the maximum packing of mineral particles, respectively. It should be noted that e is a dynamic (flow conditions dependent) quantity. For ϕ_m, we used the values obtained from the η *vs* ϕ Krieger–Dougherty fit (Section 3.3; Table 1).

The other parameter which is needed to calculate $e\phi_p^{sol}$, ϕ_p^{sol}, refers to the polymer in solution, not in the adsorbed state. Thus, in order to calculate it, the amount of adsorbed polymer has to be subtracted from the total amount of polymer introduced in the paste:

$$\phi_p^{sol} = \frac{\rho}{\rho_{pol}} \frac{(p/s) - (p^{ads^\circ}/s)}{1/\phi - 1} \tag{4}$$

In this relationship, ρ_{pol}, (p/s) and (p^{ads°/s) are the specific gravity of the polymer, the polymer over solid ratios in the paste and at the adsorption plateau, respectively.

When the relative viscosity, η_N^* or η_{pN}^*, is plotted *vs* the effective lubrication length, $e\phi_p^{sol}$, a significant simplification of the correlations is obtained. All the data points for the different polymer concentrations *p*/*w* fall on a master curve. In the cement pastes, each polymer (PA and PEO) leads to its own master curve (Fig. 16) but in the silica pastes, one single master curve is obtained gathering the data for the two polymers (Fig. 17).

All master curves exhibit two regimes. In the first regime, at low effective lubrication length, the relative viscosity is strongly and linearly (in log relative viscosity *vs* log $e\phi_p^{sol}$ representation) decreasing with $e\phi_p^{sol}$. This may be due either to an increase of the average separation, or to an increase of the polymer concentration and better lubrication. Interestingly, in three cases out of four (cement/PEO, silica/PEO and silica/PA), the exponent of the linear log–log correlation is the same: −3 ±0.25. In the cement/PA case, it is significantly larger, close to −4.5. Everything happens as if the viscosity of the dispersing fluid used to calculate the relative viscosity were too low. This might be due to some calcium-induced cross-linking of the PA polymer in the interstitial cement solution. In the second regime at large effective lubrication length, the relative viscosity becomes independent of $e\phi_p^{sol}$. In this regime, the particles are far from each other on the average and/or their approach is made difficult by the high polymer concentration.

3.5. The shear-thickening regime

Most systems (all, except silica/PA and cement/PEO at $p/w=0.143$) exhibit a shear-thickening regime at high shear rate ($>10^{-3}$ s^{-1}) above a critical volume fraction (Figs. 6 and 7). The onset of shear-thickening is characterized by critical parameters: a critical shear stress, τ_c, a

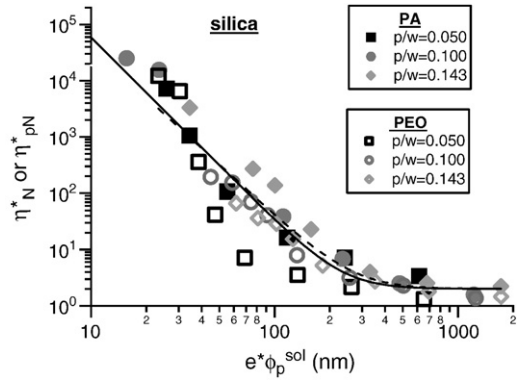

Fig. 17. Newtonian or pseudo-Newtonian relative viscosity *vs* effective lubrication length for silica pastes of varying *p*/*w* ratio containing a non-adsorbing (PA) or an adsorbing (PEO) polymer.

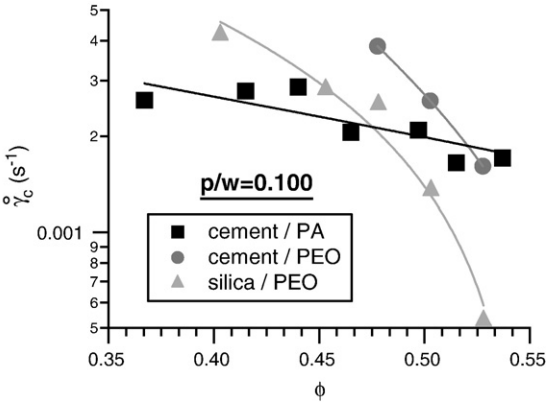

Fig. 19. Critical shear-rate at the onset of shear-thickening, $\dot{\gamma}_c$, *vs* mineral particles volume fraction, for $p/w=0.100$.

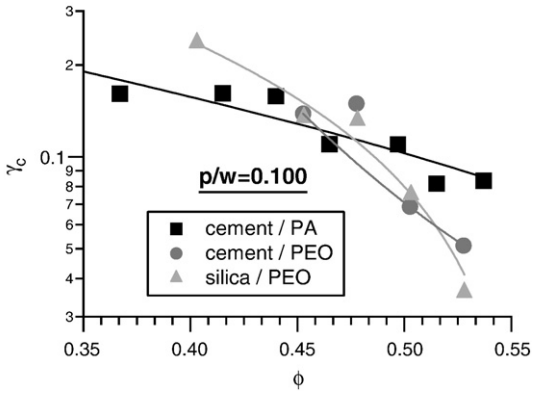

Fig. 20. Critical strain at the onset of shear-thickening, γ_c, *vs* mineral particles volume fraction, for p/w=0.100.

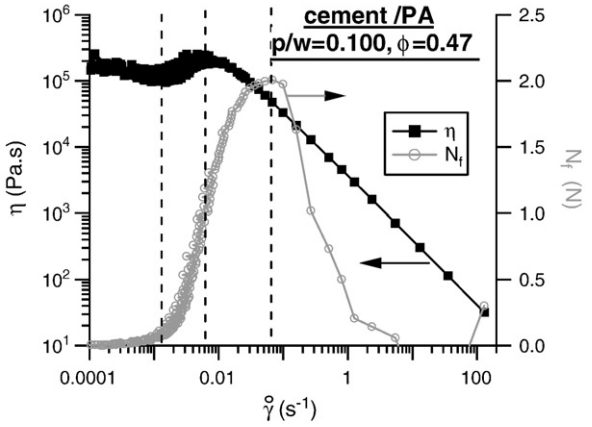

Fig. 22. Correlation between shear-thickening and normal force increase for a PA containing cement paste of p/w=0.100 and ϕ=0.47.

critical shear rate, $\dot{\gamma}_c$, and a critical strain, γ_c, while the maximum viscosity is related to a characteristic shear strain, γ_m. For a given system, τ_c increases with ϕ (Fig. 18) while $\dot{\gamma}_c$ and γ_c (as well as γ_m) decrease (Figs. 19–21). $\dot{\gamma}_c$ ranges from 10^{-3} to 5.10^{-3} s^{-1} while γ_c typically stands between 0.05 to 0.4. γ_m is of order unity.

A priori, the shear-thickening behaviour of the pastes could be an intrinsic property of the polymer solutions. It could also stem from the particle suspension, or from a combination of effects. Several arguments allow us to discard the first hypothesis. (i) Shear-thickening is observed with plain pastes. (ii) Shear-thickening occurs beyond a critical solid volume fraction only. (iii) It occurs with two very different polymers. PEO is a non-ionic linear chain, whereas PA has a polyelectrolyte backbone with short ethyl side-chains. The latter can possibly form inter-chain hydrophobic domains at high shear rate, but not the former. In cement pastes, PA could also form Ca-mediated inter-chain bridges, but not PEO. (iv) The monomer concentration is always well above the critical concentration, C*, at which the chains start to overlap [20]. (v) Shear-thickening is observed with adsorbing and non-adsorbing polymers. This allows us to rule out a mechanism involving the entanglement of chains bridging adjacent particles [21]. As a whole, all the previous points are inconsistent with a shear-thickening effect directly due to the polymer molecules in solution or to the adsorbed molecules.

As far as the dispersion of particles is concerned, several mechanisms may also be considered. In colloidal suspension, shear-thickening has been associated with order–disorder transitions or with hydrodynamic aggregate formation [22]. Direct contact chains along the compressive axis of the shear flow have also been invoked [23,24]. Order–disorder transitions are very unlikely in a paste of non-colloidal grains with no well-defined shape and a broad distribution of sizes, like the cement or silica pastes used in this work. A very meaningful observation in favour of a mechanism involving direct contact between hard objects is that the onset of shear-thickening is concomitant to an important normal force increase, N_f (Fig. 22). This may be considered as the signature of a dilatant behaviour, like in dry or wet granular media under shear (dry or wet sand for instance). In the experimental configuration used for the rheological measurements (ridged plane–plane geometry), dilatancy will unavoidably lead to material expulsion on the lateral boundary of the circular plates. As mentioned in Section 3.2, this was indeed observed.

If dilatancy is really occurring, then an extensive network of direct particle-particle contacts is involved and the basic constitutive law of sliding friction mechanics – Coulomb's law, relating the normal force to the shear force via the friction coefficient – should apply:

$$F_t = \mu N_f \tag{5}$$

In our case, the shear force to consider is the *extra* shear force, ΔF_t, due to the formation of direct contacts:

$$\Delta F_t = \mu N_f \tag{6}$$

In order to calculate ΔF_t, the shear stress due to the Newtonian flow of the paste has first to be subtracted from the total shear stress, τ. This yields the frictional stress, $\Delta\tau$, which corresponds to the frictional torque, $\Delta\Gamma$. Then, in order to calculate the *force* (torque = force × lever arm) one has to take into account the inhomogeneous

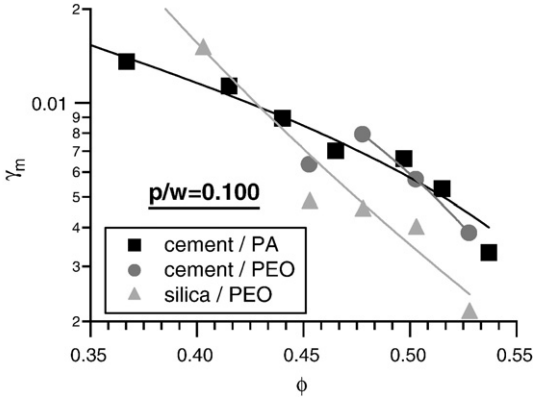

Fig. 21. Strain at maximum viscosity value, γ_m, *vs* mineral particles volume fraction, for p/w=0.100.

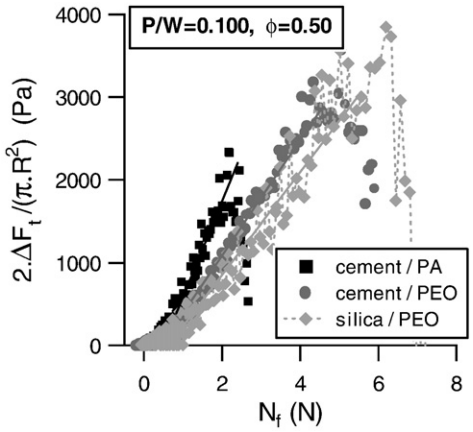

Fig. 23. Correlation between the extra-shear force, ΔF_t, and the normal force, N_f, for polymers containing pastes of p/w=0.100 and ϕ=0.50.

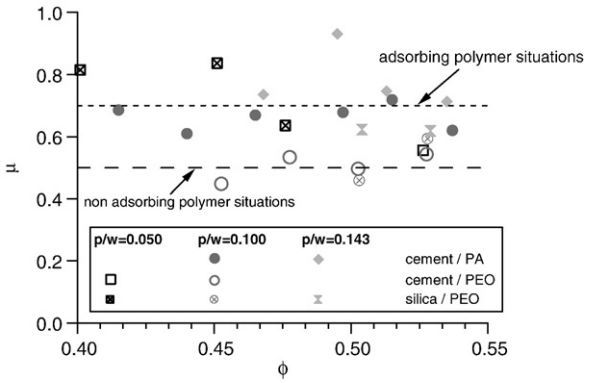

Fig. 24. Sliding friction coefficient, μ, characteristic of the shear-thickening, *vs.*

character of the shear rate in a plane-plane geometry. Only the crown of matter submitted to a shear rate greater than $\dot{\gamma}_c$ has to be considered. This crown has an inner radius r_{min} and extends up to the plane–plane radius, R. Its average radius r_m can be written as:

$$r_m = \frac{r_{min} + R}{2} = \frac{R}{2}.(1 + \dot{\gamma}_c/\dot{\gamma}) \quad (7)$$

Thus, the extra shear force writes:

$$\Delta F_t = \frac{\Delta \Gamma}{r_m} = \frac{\pi R^2}{2 r_m} \Delta \tau \quad (8)$$

The extra shear force ΔF_t has been plotted *vs* the normal force, N_f. As exemplified in Fig. 23, excellent linear relationships are obtained. This validates the idea that the phenomenon underlying the shear-thickening behavior is intergranular friction forced by the impeded dilatancy of the paste between the rheometer plateaus. The friction coefficients μ were calculated from the slopes of the previous plots. In the 22 values obtained, two groups may be identified (Fig. 24). The first group, centered on 0.5, gathers the values obtained in the non-adsorbing polymer situations. The second group, centered on 0.7, gathers the values obtained in the adsorbing polymer situations. The μ values found fall well within the range expected for "dry" ceramic-over-ceramic friction (μ=0.05 to 0.5) [25] or for "dry" polymer-over-polymer friction (μ=0.05 to 1.0) [25]. More specifically, our values are in good agreement with the values measured by K. Kendall [6] for plain cement pastes (μ=0.64 or 0.70) in capillary rheometer or plastometer experiments.

Returning now to the dependence of the characteristic shear strain at maximum viscosity, γ_m, the critical strain, γ_c, and the critical shear stress, τ_c, with respect to the solid volume fraction, ϕ, several trends or values may be readily interpreted. The average value of γ_m close to 1 can be readily explained in terms of dilatancy, since a strain of 1 in a dense monodispersed paste corresponds roughly to the motion of a particle over its nearest neighbor, in a configuration where the dilatancy effect should be at its maximum. The decrease of γ_c with ϕ is also intuitively obvious since the larger the particle concentration, the shorter the distance to encounter a neighbor. And the stress required for moving a particle over that distance will be all the larger as the paste is more concentrated and more viscous.

4. Conclusion

In agreement with our previous work on the extrusion of dense cement-polymer pastes, it was confirmed by shear rheometric measurements in plane-plane geometry that, in concentrated suspensions of non Brownian cement or silica particles, direct contact friction between particles is contributing to the overall energy dissipation. These contacts are not lubricated by the adsorbed polymer layers. Instead, it is hydrodynamic lubrication due to the interstitial solution of non adsorbed polymer which, by preventing contacts to occur, reduces the overall energy dissipation. This leads to the counter-intuitive result where, by increasing the interstitial fluid viscosity, the paste viscosity is decreased. When hydrodynamic lubrication is no longer able to avoid direct frictional contact, dilatant and shear-thickening behavior sets in. The friction coefficients calculated in this regime are in good agreement with macroscopic measurements.

References

[1] W.B. Russel, D.A. Saville, W.R. Schowalter, Colloidal Dispersions, Cambridge University Press, Cambridge, 1989.
[2] N.A. Leighton, A. Acrivos, On the viscosity of a concentrated suspension of solid spheres, Rheol. Acta 27 (1967) 847–853.
[3] P. Coussot, Mudflow Rheology and Dynamics, Balkema, Amsterdam, 1997.
[4] P. Coussot, C. Ancey, Rheophysical classification of concentrated suspensions and granular pastes, Phys. Rev., E 59 (1999) 4445–4457.
[5] F. de Larrard, Concrete Mixture Proportioning, E & FN Spon, London, 1999.
[6] K. Kendall, Interparticle friction in slurries, in: J. Briscoe, J. Adams (Eds.), Tribology in Particulate Technology, Adam Hilger, Bristol, 1987, pp. 91–102.
[7] R.J. Flatt, P. Bowen, YODEL: a yield stress model for suspensions, J. Am. Ceram. Soc. 89 (2006) 1244–1256.
[8] R.J. Flatt, P. Bowen, Yield stress of multimodal powder suspensions: an extension of the YODEL, J. Am. Ceram. Soc. 90 (2007) 1038–1044.
[9] N. Roussel, A thixotropy model for fresh fluid concretes: theory, validation and applications, Cem. Concr. Res. 36 (2006) 1797–1806.
[10] N. Roussel, R. Le Roy, P. Coussot, Thixotropy modelling at local and macroscopic scales, J. Non-Newton. Fluid Mech. 117 (2004) 85–95.
[11] H. Lombois-Burger, P. Colombet, J.-L. Halary, H. Van Damme, Kneading and extrusion in dense polymer-cement pastes, Cem. Concr. Res. 36 (2006) 2086–2097.
[12] F. Merlin, H. Guitouni, H. Mouhoubi, S. Mariot, F. Vallée, H. Van Damme, Adsorption and heterocoagulation of nonionic surfactants and latex particles on cement hydrates, J. Colloid Interface Sci. 281 (2005) 1–10.
[13] T. Zhang, S. Shang, F. Yin, A. Aishah, A. Salmiah, T.L. Ooi, Adsorptive behaviour of surfactants on surface of Portland cement, Cem. Concr. Res. 31 (2001) 1009–1015.
[14] I.M. Krieger, T.J. Dougherty, Trans. Soc. Rheol. 3 (1959) 137–152.
[15] G.K. Bachelor, An Introduction to Fluid Dynamics, Cambridge University Press, Cambridge, 1967, pp. 246–253.
[16] S. Mansoutre, P. Colombet, H. Van Damme, Water retention and granular rheological behavior of fresh C3S paste as function of concentration, Cem. Concr. Res. 29 (1999) 1441–1453.
[17] P. Coussot, Rheometry of Pastes, Suspensions, and Granular Materials, John Wiley & Sons, Hoboken, 2005 chap. 2, Rheophysics of Pastes and Granular Materials.
[18] M.A. Schultz, L.J. Struble, Use of oscillatory shear to study flow behavior of fresh cement, Cem. Concr. Res. 23 (1993) 272–282.
[19] L.J. Struble, M.A. Schultz, Using creep and recovery to study flow behavior of fresh cement paste, Cem Concr Res 23 (1993) 1369–1379.
[20] P.G. de Gennes, Scaling Concepts in Polymer Physics, Cornell University Press, 1979.
[21] F. Lafuma, K. Wong, B. Cabane, Bridging colloidal particles through adsorbed polymers, J. Collloid Interface Sci. 143 (1991) 9–21.
[22] R.L. Hoffman, Explanations for the cause of shear thickening in concentrated colloidal dispersions, J. Rheol. 42 (1998) 111–123.
[23] M.E. Cates, J.P. Wittmer, J.P. Bouchaud, Jamming, force chains, and fragile matter, Phys. Rev. Lett. 81 (1998) 1841–1844.
[24] D. Lootens, H. Van Damme, P. Hébraud, Giant stress fluctuations at the jamming transition, Phys. Rev. Lett. 90 (2003) 178301.
[25] M.F. Ashby, D.R.H. Jones, Friction and Wear, in Materials I. Properties and Applications, Dunod, Paris, 1998.